

Article

Anticancer Effects of Fucoxanthin in a PDX Model of Advanced Stage Pancreatic Cancer with Alteration of Several Multifunctional Molecules

Masaru Terasaki ^{1,2,*} , Sally Suzuki ¹, Takuji Tanaka ³ , Hayato Maeda ⁴ , Masaki Shibata ⁴, Kazuo Miyashita ⁵, Yasuhiro Kuramitsu ², Junichi Hamada ², Tohru Ohta ², Shigehiro Yagishita ⁶, Akinobu Hamada ⁶ , Yasunari Sakamoto ⁷, Susumu Hijioka ⁷ , Chigusa Morizane ⁷ and Mami Takahashi ⁸ 

- ¹ School of Pharmaceutical Sciences, Health Sciences University of Hokkaido, 1757 Kanazawa, Ishikari-Tobetsu 061-0293, Japan; s181081@hoku-iryu-u.ac.jp
 - ² Advanced Research Promotion Center, Health Sciences University of Hokkaido, 1757 Kanazawa, Ishikari-Tobetsu 061-0293, Japan; climates@hoku-iryu-u.ac.jp (Y.K.); jun1hamada@hoku-iryu-u.ac.jp (J.H.); ohta@hoku-iryu-u.ac.jp (T.O.)
 - ³ Department of Diagnostic Pathology and Research Center of Diagnostic Pathology, Gifu Municipal Hospital, 7-1 Kashima-cho, Gifu City 500-8513, Japan; takutt@gmhosp.gifu.gifu.jp
 - ⁴ Faculty of Agriculture and Life Science, Hirosaki University, 3 Bunkyo-Cho, Hirosaki City 036-8561, Japan; hayatosp@hirosaki-u.ac.jp (H.M.); iu3222004@hirosaki-u.ac.jp (M.S.)
 - ⁵ Hokkaido Bunkyo University, 5-196-1 Kogane-Chuo, Eniwa City 061-1449, Japan; kmiyashita@do-bunkyo.ac.jp
 - ⁶ Division of Molecular Pharmacology, National Cancer Center Research Institute, 5-1-1 Tsukiji, Chuo-ku, Tokyo 104-0045, Japan; syagishi@ncc.go.jp (S.Y.); akhamad@ncc.go.jp (A.H.)
 - ⁷ Department of Hepatobiliary and Pancreatic Oncology, National Cancer Center Hospital, 5-1-1 Tsukiji, Chuo-ku, Tokyo 104-0045, Japan; yasakamo@ncc.go.jp (Y.S.); shijioka@ncc.go.jp (S.H.); cmorizan@ncc.go.jp (C.M.)
 - ⁸ Central Animal Division, National Cancer Center Research Institute, 5-1-1 Tsukiji, Chuo-ku, Tokyo 104-0045, Japan; mtakahas@ncc.go.jp
- * Correspondence: terasaki@hoku-iryu-u.ac.jp; Tel.: +81-133-23-1211



Citation: Terasaki, M.; Suzuki, S.; Tanaka, T.; Maeda, H.; Shibata, M.; Miyashita, K.; Kuramitsu, Y.; Hamada, J.; Ohta, T.; Yagishita, S.; et al. Anticancer Effects of Fucoxanthin in a PDX Model of Advanced Stage Pancreatic Cancer with Alteration of Several Multifunctional Molecules. *Onco* **2023**, *3*, 217–236. <https://doi.org/10.3390/onco3040016>

Academic Editors: Youngchul Kim and Constantin N. Baxevanis

Received: 1 August 2023

Revised: 22 September 2023

Accepted: 22 September 2023

Published: 24 September 2023



Copyright: © 2023 by the authors. Licensee MDPI, Basel, Switzerland. This article is an open access article distributed under the terms and conditions of the Creative Commons Attribution (CC BY) license (<https://creativecommons.org/licenses/by/4.0/>).

Simple Summary: Fucoxanthin (Fx) is a representative marine carotenoid. To achieve clinical application of Fx toward cancer treatment, it is important to clarify the presence or absence of its effect in patient-derived xenograft (PDX) mice. Here, we investigated the anticancer effects of Fx in pancreatic cancer (PC)-PDX mice. Consequently, our results suggest that the increase in decorin (DCN) and pro-oxidant p-p38(Thr¹⁸⁰/Tyr¹⁸²) and phospho c-Jun N-terminal kinase (pJNK)(Thr¹⁸³/Tyr¹⁸⁵)-related signals and the inhibition of insulin growth factor binding protein 2 (IGFBP2)-, epithelial cell adhesion molecule (EpCAM)-, and lipocalin 2 (LCN2)-related signals are key regulators of tumor suppression in the PC-PDX mice. The protein alterations in the mice were partially supported by in vitro experiments. Therefore, Fx may be a promising candidate for cancer therapy in patients with PC.

Abstract: Pancreatic cancer (PC) is one of the most fatal cancers, and there is an urgent need to develop new anticancer agents with fewer side effects for the treatment of this condition. A patient-derived xenograft (PDX) mouse model transplanted with cancer tissue from patients is widely accepted as the best preclinical model for evaluating the anticancer potential of drug candidates. Fucoxanthin (Fx) is a highly polar carotenoid contained in edible marine brown algae and possesses anticancer activity. However, there is a lack of data on the effects of Fx in PDX models. We investigated the anticancer effects of Fx in PDX mice transplanted with cancer tissues derived from a patient with PC (PC-PDX) using comprehensive protein expression assay. Fx administration (0.3% Fx diet) ad libitum for 27 days significantly abrogated tumor development (0.4-fold) and induced tumor differentiation in PC-PDX mice, as compared to those in the control mice. Fx significantly upregulated the expression of non-glycanated DCN (2.4-fold), tended to increase the expressions of p-p38(Thr¹⁸⁰/Tyr¹⁸²) (1.6-fold) and pJNK(Thr¹⁸³/Tyr¹⁸⁵) (1.8-fold), significantly downregulated IGFBP2 (0.6-fold) and EpCAM (0.7-fold), and tended to decrease LCN2 (0.6-fold) levels in the tumors of the PC-PDX mice, as compared to

those in the control mice. Some of the protein expression patterns were consistent with the in vitro experiments. That is, treatment of fucoxanthinol (FxOH), a prime metabolite derived from dietary Fx, enhanced non-glycanated DCN, p-p38(Thr¹⁸⁰/Tyr¹⁸²), and pJNK(Thr¹⁸³/Tyr¹⁸⁵) levels in human PC PANC-1 and BxPC-3 cells. These results suggested that Fx exerts anticancer and differentiation effects in a PC-PDX mice through alterations of some multifunctional molecules.

Keywords: anticancer effect; fucoxanthin; patient-derived xenograft; pancreatic cancer; decorin; heme oxygenase 1; insulin growth factor binding protein 2; lipocalin 2; epithelial cell adhesion molecule

1. Introduction

Pancreatic cancer (PC) is a malignant neoplasm known to be associated with some of the most fatal outcomes worldwide. The incidence of PC is closely related to high mortality rates. According to the GLOBOCAN 2020 database reports, PC accounts for 495,773 new cancer cases and is responsible for 466,003 cancer-related deaths worldwide [1]. In the United States of America, the number of new cases and deaths due to PC is expected to continue to increase until 2040 [2]. It is estimated that the five-year relative survival rates of PC at localized, regional, and distant stages are 44%, 15%, and 3%, respectively (combined survival rates of all stages = 12%) [3]. Growing evidence suggests that high-risk factors for PC include smoking, adult obesity, adult attained height, type 2 diabetes mellitus, chronic pancreatitis, certain chemicals, age (>45 years), sex (with males having a higher risk than females), race, family history, gene mutations, infections, and the consumption of certain foods and drinks. Definitive evidence regarding decreased risk factors for PC is yet to be established. However, certain lifestyle-related improvements are recommended for PC prevention, such as smoking cessation, maintaining appropriate body weight, habitual exercise, and the intake of vegetables, fruits, and whole grains [3,4].

It is difficult to completely eliminate PC using chemotherapies, such as gemcitabine, 5-fluorouracil, and albumin-bound paclitaxel, which are mostly used to prolong survival. In addition, there are very few anticancer drugs that can be used for PC chemotherapy, and the side effects upon administration of these drugs must also be considered [3]. Therefore, there is an urgent need to develop new anticancer drugs that can treat PC with fewer side effects, prior to other cancers.

Pancreatic ductal adenocarcinoma (PDAC) is the dominant histological type of PC (approximately 90% of all PC cases) [5]. Pancreatic intraepithelial neoplasias (PanINs) are preinvasive lesions that occur at the onset of PDAC, and their progression is classified into four types from early to late. Somatic mutations in Kirsten ras (*KRAS*), cyclin-dependent kinase inhibitor 2A (*CDKN2A*), tumor protein 53 (*TP53*), mothers against decapentaplegic homolog 4 (*SMAD4*), breast cancer susceptibility gene 1 (*BRCA1*), and *BRCA2* are frequently associated with PanIN progression and have been suggested to trigger PDAC onset [5,6].

Several animal models of PDAC have been developed. A mouse model of PDAC with *Kras* mutation (*Ptf1a*^{Cre/+}; *LSL-K-ras*^{G12D/+} mice) shows PanIN progression and develops pathological PDAC resembling human PDAC [7]. Moreover, *Ptf1a*^{Cre/+}; *LSL-K-ras*^{G12D/+} mice combined with *Tgfb2* knockout or *Trp53*^{R172H} mice have been shown to exhibit a higher frequency of PDAC onset than the initial *Ptf1a*^{Cre/+}; *LSL-K-ras*^{G12D/+} mice [8,9]. Treatment of Syrian golden hamsters with *N*-nitrosobis(2-oxopropyl)amine (BOP) was found to induce PanIN, with the occurrence of PDAC found to be associated with genetic mutations in *Kras*, *cdkn2a*, and *smad4* [10]. Currently, patient-derived xenograft (PDX) models with directly transplanted tissues from cancer patients have been recognized as the best models for evaluating the anticancer potential of drug candidates, replacing in vitro and in vivo models that use the US National Cancer Institute-60 panel, which is a fundamental tool comprising 60 human cancer cell lines [11,12]. Engrafted cancers can conserve the histopathological features and molecular regulation of patient-derived cancer tissues. PDX has been suggested as an optimal model for assessing anticancer

drugs, exhibiting 90% of the overall predictive accuracy of clinical therapeutic efficacy in patients [13,14]. However, the anticancer effects of general foods and food-derived functional compounds in PDX models remain poorly understood.

Fucoxanthin (Fx) is a highly polar carotenoid predominantly present in edible marine brown algae. The Fx molecule ($C_{42}H_{58}O_6$, 658.9 g/mol) comprises a polyene chain, an allenic bond, a 5,6-monoepoxide group, and a carbonyl group (Supplementary Figure S1). Toxicological and interventional studies have suggested that Fx is a safe compound with no adverse effects in humans or rodents [15–20]. Fx is easily converted into deacetylated fucoxanthinol (FxOH) in the intestines of humans and mice and FxOH is one of the main metabolites detected in blood and tissues [21,22]. No clinical or epidemiological examinations of the anticancer effects of Fx and FxOH have been conducted yet. However, it has been demonstrated using *in vitro* and *in vivo* experiments that Fx and FxOH can exert the anticancer effects on colorectal, skin, duodenal, liver, lung, and breast cancers [23–26]. In addition, we revealed that Fx and FxOH have anticancer activities against a few PC *in vitro* and *in vivo* PC models. FxOH treatment (5.0 μ M) could promote apoptosis in a mouse PDAC cell line (KMPC44) established from the *Ptfla*^{Cre/+}; *LSL-Kras*^{G12D/+} mice and a hamster PDAC cell line (HaPC-5) established from the BOP-treated Syrian golden hamster [27,28]. Furthermore, Fx administration (488.8 mg/Fx/kg body weight [bw]/mouse/day) could substantially inhibit the onset of PDAC in a PDAC mouse (C57BL/6J) model with allogenic and orthotopic transplantations of the KMPC44 cells [29]. Lu et al. showed that Fx boosted the growth inhibitory effects of gemcitabine in human PC PANC-1 and MIA PaCa-2 cells [30]. Fx may be a promising candidate that contributes to prolonging the survival of patients with PC in the future. Considering its clinical application, it is necessary to investigate the effects of Fx in PDX models inoculated with PC tissues (PC-PDX).

In this study, we examined the anticancer potential of Fx in a PC-PDX mouse model.

2. Materials and Methods

2.1. Chemical

An Fx-enriched oil (5.0 *w/v* % Fx-oil; product name, Fucoxanthin-5KW[®]) predominantly comprising palm oil and minor ingredients (proteins, carbohydrates, and sodium) was kindly supplied by Oryza Oil & Fat Chemical Co., Ltd. (Aichi, Japan). Palm oil without Fx was used as the control oil. All-*trans*-FxOH (purity, $\geq 98\%$) was purified from marine algal lipids by Dr. Hayato Maeda (Hirosaki University, Japan). Dimethyl sulfoxide (DMSO) (cat.no. 041-07217), formaldehyde (37%) (cat.no. A16163) and (10%) (cat.no. 060-01667), Hank's balanced salt solution (HBSS) (cat.no. 082-08961), isoflurane (cat.no. 099-06571), and poly(oxyethylene 20 sorbitan) monolaurate (Tween 20) (cat.no. 166-21213), and Roswell Park Memorial Institute -1640 cell culture medium (RPMI) (cat.no. 183-02165) were obtained from FUJIFILM Wako Pure Chemicals (Osaka, Japan). RNAlater (cat.no. AM7021), GlutaMAX (cat.no. 35050061), fetal bovine serum (FBS) (cat.no.10437), and penicillin/streptomycin (antibiotics) (cat.no.15140122) were purchased from Thermo Fisher Scientific (Waltham, MA, USA). Bovine serum albumin (BSA) (cat.no. 01281-97) was obtained from Nacalai Tesque (Kyoto, Japan), respectively. The sources, catalog numbers, and brand names of the primary antibodies are listed in Supplementary Table S1. Goat anti-rabbit (cat.no. #7074) and anti-mouse (cat.no. SA00001-1) secondary antibodies conjugated with horseradish peroxidase (HRP) were purchased from Cell Signaling Technology (Danvers, MA, USA) and Proteintech (Rosemont, IL, USA), respectively, and 4',6'-Diamidino-2-phenylindole (DAPI) (cat.no. 340-07971) was purchased from Dojindo (Kumamoto, Japan). All the other chemicals and solvents were of analytical grade.

2.2. Establishment of PDX Tumor from Human PC Tissue

The J-PDX library was created in 2018 for Japanese patients with cancer, as described previously [31]. More than 1000 patients with cancer were provided with sufficient opportunities to reject study participation at the National Cancer Center Hospital in Japan. The

patients signed an informed consent form and agreed to participate in the sample collection and data transmission. This study was approved by the Institutional Review Board of the National Cancer Center (identification code, 2015-123 and 2021-163; authorization, 2015 and 2021). Samples isolated from various departments, such as surgical specimens, needle biopsies, endoscopy, and ascitic fluids, were rapidly soaked in storage solution, transiently stored at 4 °C, and conveyed to an adequate facility for multi-omics analyses or PDX establishment.

We selected a patient with PC from the J-PDX library based on the following characteristics: race, age, sex, and location of sample collection. In addition, we considered clinical characteristics such as disease, pathological type, tumor-node-metastasis (TNM) status, clinical stage, and prior treatment history (chemotherapy, radiotherapy, and immunotherapy) of the primary cancer tissue. DNA and RNA were extracted from the tumor sample using a KingFisher Cell and Tissue DNA Kit (cat.no. 97030196) (Thermo Fisher Scientific, Waltham, MA, USA) and MagMAX mirVana Total RNA Isolation Kit (A27828) (both from Thermo Fisher Scientific, Waltham, MA, USA), respectively. Hotspots, fusions, and copy number variations of 161 cancer genes in the tumor sample were assessed using a rapid next-generation sequencer (OncoPrint Comprehensive Assay v3 with the Ion Torrent Genexus System (software version 6.6 and cat.no. A46296); Thermo Fisher Scientific, Waltham, MA, USA).

To establish the PC-PDX mice, we transplanted tumor tissues from a patient with PC into mice as follows: Female NOD.Cg-Prkdc^{scid} Il2rg^{tm1Sug}/ShiJic (NOG) mice (5 weeks old) were purchased from In-Vivo Science (Kanagawa, Japan). The mice were housed in polycarbonate cages in a humidity- and temperature-controlled room under a 12 h light/dark cycle. PC tissue was cut into 2 mm³ sections and subcutaneously inoculated into the flank region of 6-week-old mice using a transplantation needle, to generate PC-PDX mice. The estimated tumor size was monitored weekly and determined using the following formula: $a \text{ (mm)} \times b^2 \text{ (mm)} / 2$ (a , long range; b , short range). Tumor passage was performed when the tumor size reached 200–2000 mm³. The tumor established in the first PC-PDX mouse was named TG₁. The second- and third-passage tumors that developed in other PDX mice were named TG₂ and TG₃, respectively [31]. Animal experiments were conducted according to the guidelines of the Institute for Laboratory Animal Research, National Cancer Center Research Institute (identification codes: T17-020, T17-073, and T19-008; authorizations 2017 and 2021). Mice used for tumor passage were euthanized under 2% isoflurane inhalation (air, 2.0 L/min). In the present study, we used TG₃ tissue from the selected patient with PC, provided by the National Cancer Center J-PDX library in Japan.

2.3. Animal Experiments

Female CB17.Cg-Prkdc^{scid} Lyst^{bg-J}/CrJcrlj (SCID-Beige) mice (4 weeks old) were purchased from Oriental Yeast (Tokyo, Japan), placed in plastic cages with sterilized softwood chips, and maintained under constant temperature, humidity, and a 12 h light/dark cycle. The mice received standard solid MF chow (Oriental Yeast, Tokyo, Japan) and tap water ad libitum. After one week of acclimatization, three pieces of TG₃ PC tissue (2 mm³) were subcutaneously injected into the flank region of the 5-week-old mice using a transplantation needle (to generate TG₄-PC-PDX). The mice were monitored daily for clinical signs. After three months, the mice were euthanized under 2% isoflurane anesthesia (air, 2.0 L/min), and harvested tumor tissues were cut into 36 pieces (2 mm³ in size) under HBSS (4 °C) to generate TG₅-PC-PDX mice.

Female SCID-Beige mice (4 weeks old, 27 mice) were purchased from Oriental Yeast (Tokyo, Japan), randomly divided into plastic cages with sterilized softwood chips (three mice/cage), and kept under constant temperature, humidity, and a 12 h light/dark cycle. The mice received standard solid MF chow (Oriental Yeast, Tokyo, Japan) and tap water ad libitum. After one week of acclimatization, two pieces of the TG₄ PC tissues (2 mm³) from the TG₄-PC-PDX mouse were subcutaneously injected into the flank region of each

mouse (5 weeks old) using a transplantation needle (to generate TG₅-PC-PDX) on day 0 (5-week-old). Fx-oil was painted on a solid MF at a concentration of 0.3% Fx (3.0 mg Fx/g MF chow, Fx-high diet) and 0.1% Fx (1.0 mg Fx/g MF chow, Fx-low diet). The control diet comprised of solid MF with an equivalent volume of control oil (control diet). The mice were assigned to the Fx-high diet (Group 1, *n* = 9), Fx-low diet (Group 2, *n* = 9), and control diet (Group 3, *n* = 9) groups, which were administered Fx-high, Fx-low, and control diets ad libitum for 27 days (days 0–27), until sacrifice. The body weight, estimated tumor size, and other clinical features of the mice were regularly monitored. The estimated tumor size (mm³) was determined using the following formula given above. TG₅-PC-PDX mice in Groups 1–3 were euthanized under 2% isoflurane anesthesia (air, 2.0 L/min), and whole flank tumors of each mouse were excised, washed with cold phosphate-buffered saline (PBS), and cut into several pieces. For histopathological assessment, one piece of the tumor was fixed in 10% neutral buffered formalin for 2 days. Hematoxylin and eosin (HE)-stained sections were prepared using Morphotechnology (Hokkaido, Japan). Other tumor pieces were permeabilized with RNAlater (500 µL) overnight at 4 °C and then were frozen at –80 °C until proteome and western blot analyses. An expert pathologist performed a histopathological diagnosis of the tumors. The study protocol was approved to be an operational project by the Institutional Review Board of the National Cancer Center Research Institute (identification code, 2021-163; authorization, 2021) and of the Health Sciences University of Hokkaido (identification code, 21P003; authorization, 2021). The animal experiments were approved by the Institutional Guidelines for Animal Care and Use of the Health Sciences University of Hokkaido, in accordance with the “Guidelines for Animal Experiments in the Health Sciences University of Hokkaido” (identification code, 22-003; authorization, 2021).

2.4. Proteome Analysis

Whole tumors were lysed in a lysis buffer and sonicated. The total protein content was measured using the Bradford assay, followed by denaturation at 95 °C for 5 min. Total proteins from Fx-high diet-treated mice (group 1) or control mice (group 3) were prepared as a sample with equivalently mixed proteins (total 75 µg) and then subjected to proteome analysis. Protein samples were purified, lysed, denatured, alkylated, and digested with trypsin, and part of them (200 ng) were applied to quantitative liquid chromatography with tandem mass spectrometry (UltiMate 3000 RSLC Nano LC System) using a Q Exactive HF-X mass spectrometer (both from Thermo Fisher Scientific, Carlsbad, CA, USA) at the Kazusa DNA Research Institute (Chiba, Japan) (analysis registration number: KK1583). Proteome profiles based on the mass spectroscopy data were analyzed using Scaffold DIA software (Promega Software, Portland, OR, USA). The protein sequence database was based on the Human UniProtKB/Swiss-Prot database and the ProSIT spectral library (<https://www.proteomicsdb.org/prosit/>) (accessed and downloaded on 26 November 2021). The quantitative value corresponding to the protein expression was calculated for proteins satisfying both cutoff peptide false discovery rate (FDR) ($\leq 1.0\%$) and protein FDR ($\leq 1.0\%$).

2.5. Cell Proliferation Assay

Two human PC cell lines, PANC-1 (ATCC no. CRL-1469) and BxPC-3 (ATCC no. CRL-1687), were purchased from American Type Culture Collection (Manassas, VA, USA). The cells were routinely cultured in RPMI-1640 medium with 10% heat-inactivated FBS, 1% GlutaMAX™, 40,000 U/L penicillin, and 40 mg/L streptomycin (10%FBS/RPMI) at 37 °C in a humidified atmosphere containing 95% air and 5% CO₂ until use. Briefly, PANC-1 and BxPC-3 cells were seeded into a 24-well plate (at a density of 5×10^4 cells/mL) with 10% FBS/RPMI for one day. The cells were incubated in 10% FBS/RPMI with FxOH (final concentrations of 5 and 20 µM) or vehicle alone (DMSO) for 2 days. The cells were washed with PBS and fixed in 10% formalin in PBS (1:1) for 10 min, at 37 °C. The cells were then washed and incubated with PBS. Following that, DAPI solution in PBS was added to the

cells and incubated for 10 min at 37 °C. A Keyence BZ-X810 microscope (Osaka, Japan) was used to observe and acquire images of the cellular nuclei. The total area of the blue-stained nuclei was quantified using Keyence BZ-X810 analysis software BZ-H4AS (Osaka, Japan).

2.6. Western Blot Analysis

Western blot analysis of the tumors was performed as described previously [29]. Whole tumors were harvested from Groups 1 and 3 and sonicated in a lysis buffer. PANC-1 and BxPC-3 cells were seeded into 10 cm plates at a density of 5×10^4 cells/mL and allowed to adhere for 1 day. The cells were then exposed to 10% FBS/RPMI with FxOH (final concentrations of 5 and 20 μ M) or vehicle alone (DMSO), for 1 day. The cells were trypsinized, washed with PBS, and lysed using a lysis buffer. The protein content in each PDX tumor or cell line was determined using the Bradford assay. The proteins (10 μ g) in each mouse tumor or cell were subjected to 10% sodium dodecyl sulfate-polyacrylamide gel electrophoresis (SDS-PAGE) and then transferred onto Hybond polyvinylidene fluoride membranes (cat.no. 10600058) (Amersham Biosciences, Little Chalfont, UK). The PVDF membranes were blocked with Tris-buffered saline containing 0.1% Tween 20 and 1 w/v% BSA (1% BSA/TBS-T) at room temperature for 1 h, followed by incubation with each primary antibody (diluted 1:1000) in 1% BSA/TBS-T at 4 °C overnight. The membranes were then incubated with horseradish peroxidase-conjugated anti-mouse or anti-rabbit secondary antibodies (diluted 1:5000) in TBS-T at room temperature for 1 h. The protein bands were visualized using enhanced chemiluminescence (cat.no. WBKLS0500; Millipore, Billerica, MA, USA), normalized to β -actin expression as a loading control, and then quantified in comparison with a control group using Fiji ImageJ2 software (version 2.9.0/1.53t) (National Institutes of Health, <http://rsb.info.nih.gov/ij/>) (accessed on 20 October 2022).

2.7. Statistics Analysis

All results are presented as mean \pm standard error (SE). Statistical differences in tumor incidence between the two groups were assessed using Fisher's exact probability test. The normality of the distribution of the results was analyzed using the Shapiro–Wilk test. Comparisons between two groups with and without normal distribution were performed using post hoc Student's *t*-test (parametric) or Mann–Whitney *U*-test (nonparametric), respectively. In addition, comparisons among three groups with and without normal distribution were performed using one-way ANOVA (parametric) with post hoc Tukey test or Kruskal–Wallis test (nonparametric) with post hoc Dunn–Bonferroni test, respectively. The statistical analysis was conducted using SPSS Statistics version 25 (IBM Co., Ltd., Armonk, NY, USA). Differences were considered statistically significant at * $p < 0.05$ and ** $p < 0.01$.

3. Results

3.1. Characteristics of a Tumor Derived from a Patient with PC

Table 1 summarizes the basic and pathological characteristics of a patient with PC. The race, age, sex, and location of the sample collection were Japanese, in their early 70s, male, and pancreatic, respectively. The tumor characteristics were as follows: disease, primary PC without metastasis or recurrence; pathological type, adenocarcinoma (ADC); tumor node-metastasis (TNM) status, T4N1M1; clinical stage, stage IV; prior treatment history (chemotherapy, radiotherapy, and immunotherapy), none. Multi-omics analyses of 161 gene alterations in the tumor sample passaged three times in the PDX mice, named transgeneration 3 (TG₃, generally called F₃), detected hotspot mutations of *TP53* and *KRAS*, with truncating mutations of *ARID1A* and Notch Homolog 2 N-terminal-like C (*NOTCH2NLC*): *TP53*, C238Y; *KRAS*, G12D; *ARID1A*, I1816S fs Ter 67; *NOTCH2NLC*, amino acid change not identified (Supplementary Table S2). No gene fusions or copy number variations were observed among the 161 genes.

Table 1. Characteristics of the patient with pancreatic cancer.

Classification	Characteristics
Registration number	X130068
Race	Japanese
Age (years)	Early 70s
Gender	Male
Location of sample collection	Pancreas
Disease	Primary pancreatic cancer without recurrence
Pathological type	Adenocarcinoma
TNM status	T4N1M1
Clinical stage	Stage IV
Chemotherapy, radiotherapy and immunotherapy	None

3.2. Anticancer Effect of Fx Administration on the PC-PDX Mice

An Fx diet (0.3% and 0.1%) was administered to the PC-PDX mice ad libitum for 27 days. No clinical signs of disease were observed in Groups 1–3 during the experimental period. In addition, there were no significant differences in the intake amounts of the Fx-high diet-administered mice (Group 1), the Fx-low diet-administered mice (Group 2), and the control diet (Group 3) administered mice (data were assessed using the Shapiro–Wilk test, and one-way ANOVA with post hoc Tukey test): Group 1, 163.9 ± 4.6 g Fx diet/kg bw; Group 2, 177.7 ± 4.2 g Fx diet/kg bw; Group 3, 174.8 ± 4.3 g control diet/kg bw. The average Fx intakes in Groups 1 and 2 were 491.8 and 177.7 mg Fx/kg bw, respectively. There was no significant difference between the average liver weight ratio of Groups 1 and 3: Group 1, $6.3 \pm 0.2\%$ /bw; Group 3, $5.9 \pm 0.2\%$ /bw (data were assessed using Shapiro–Wilk test and Student's *t*-test). The mean bw did not differ significantly among the three groups, except for between Groups 2 and 3 on day 23 (Figure 1A). The estimated tumor sizes in Groups 1 and 2 were significantly reduced and/or tended to be lower, respectively, as compared to that of Group 3 on day 27: Group 1, 53.6 ± 15.2 mm³ (0.4-fold vs. Group 3); Group 2, 92.2 ± 28.6 mm³ (0.7-fold vs. Group 3); Group 3, 138.9 ± 28.6 mm³ (Figure 1B). However, the tumor sizes of Groups 1–3 differed minimally during most of the experimental period (days 0–23), except for on day 27. Based on the pathological diagnoses, well to moderately differentiated ADC and moderately to poorly differentiated ADC in Group 1 were significantly increased and decreased, respectively, when compared to that in Group 3, although little difference in moderately differentiated ADC was observed between Groups 1 and 3 (Supplementary Figure S2 and Supplementary Table S3).

3.3. Comprehensive Proteome Alteration in the Tumor Tissue of PDX Mice after Fx Administration

We aimed to elucidate the molecular mechanisms underlying the anticancer and differentiation-inducing effects of Fx on the tumors of PC-PDX mice, focusing particularly on the proteome profile of the tumors. Proteome analysis demonstrated that 318 upregulated (≥ 1.5 -fold) and 887 downregulated (≤ -1.5 -fold) proteins (total, 1205 proteins) were altered in the Fx-high diet-administered PDX mice, as compared to the control mice. From the molecular functions and interactions regarding cancer based on some available studies (32–36), three upregulated proteins, including the tumor suppressors of decorin (DCN) (2.6-fold) and FAF1 (1.8-fold), and a stress-inducible protein of heme oxygenase 1 (HO1) (2.5-fold) were detected as molecules that may contribute to anticancer and stress signals in the Fx-treated mice, with the top 50 upregulated proteins (Supplementary Table S4). Similarly, 109 downregulated proteins were detected as molecules that may contribute to cancer development in the mice, from the molecular functions and interactions regarding cancer. Of these, we have noted on the 24 downregulated proteins as follows: INSR (N.D., not detected compared to the that of control mice), BAG1 (N.D.), ITGB3 (N.D.), IGFBP3 (−4.0-fold), ITGA1 (−3.6-fold), LAMA5 (−3.2-fold), NECTIN2 (−3.1-fold), ECM1 (−3.0-fold), HNF4A (−2.7-fold), NFKB1 (−2.4-fold), NFKB2 (−2.3-fold), CLU (−2.3-fold),

insulin growth factor binding protein 2 (IGFBP2) (−2.3-fold), ITGA3 (−1.9-fold), COL17A1 (−1.9-fold), CD44 (−1.9-fold), CDC42EP5 (−1.8-fold), TIMP1 (−1.8-fold), lipocalin 2 (LCN2) (−1.8-fold), ADAM17 (−1.7-fold), MDK (−1.7-fold), epithelial cell adhesion molecule (EPCAM) (−1.7-fold), DAG1 (−1.7-fold), and MUC5AC (−1.6-fold), (Supplementary Table S5). Supplementary Tables S4 and S5 also show other molecules that are expected to be involved in the anticancer effects, in addition to the molecules selected above (proteins colored gray in Supplementary Tables S4 and S5). However, we could not perform subsequent western blot analysis on all the upregulated and downregulated proteins shown in Supplementary Tables S4 and S5. Thus, we proceeded with the understanding that the experimental limitations may have hindered the findings of this study.

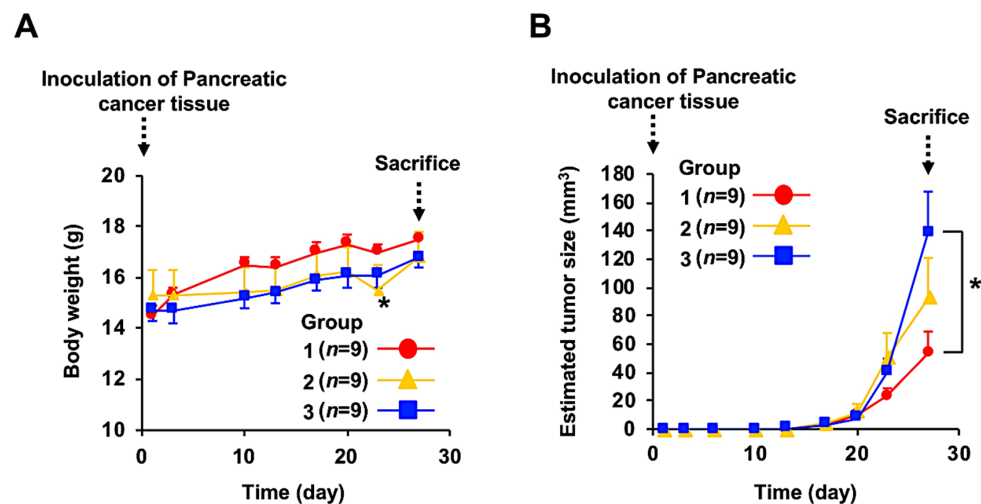


Figure 1. The growth inhibitory effect of fucoxanthin (Fx) administration on tumors of pancreatic cancer tissue-transplanted patient-derived xenograft (PC-PDX) mice. Mice in Groups 1 (red dots), 2 (yellow dots), and 3 (blue dots) were administered Fx-high, Fx-low, and control diets, respectively, ad libitum for 27 days, until sacrifice. The body weight and estimated tumor size of the PC-PDX mice were routinely measured in PC-PDX mice. **(A)** Body weight changes during the experimental period. Data are presented as the mean \pm standard error (SE) ($n = 9$). After the normality distribution of the results was checked by means of the Shapiro–Wilk test, comparisons among Groups 1–3 were performed using one-way analysis of variance with post hoc Tukey test. A statistically significant difference of $* p < 0.05$ was found between Groups 2 and 3 on day 23 only). **(B)** The subcutaneous estimated tumor size in PC-PDX mice during the experimental period, calculated based on the following formula: $a \text{ (mm)} \times b^2 \text{ (mm)} / 2$ (a , long range; b , short range). Data are presented as the mean \pm standard error (SE) ($n = 9$). After the normality distribution of the results was checked using the Shapiro–Wilk test, comparisons among Groups 1–3 were performed using Kruskal–Wallis with post hoc Dunn–Bonferroni test. A statistically significant difference of $* p < 0.05$ was found between Groups 1 and 3 on day 27).

3.4. Altered Protein Expression or Activation in the Tumor Tissues of PDX Mice after Fx Administration Based on Proteome Analyses

Based on proteome alterations, the effect of the Fx-high diet administration on the expression and activation of each selected protein (total 31 molecules based on the proteins colored gray in Supplementary Tables S4 and S5) was examined in whole tumor tissues of PC-PDX mice, using western blot analysis. Compared to the expression levels in Group 3, administration of the Fx-high diet in Group 1 significantly increased the expression of non-glycated DCN (2.4-fold), tended to increase HO1 expression (1.5-fold without statistically significant difference), significantly decreased IGFBP2 (0.6-fold) and EPCAM (0.7-fold) expression, and tended to decrease LCN2 expression (0.6-fold without statistically significant difference). Little change or appearance was observed in the expression levels of the other 32 proteins between Groups 1 and 3 (Figure 2).

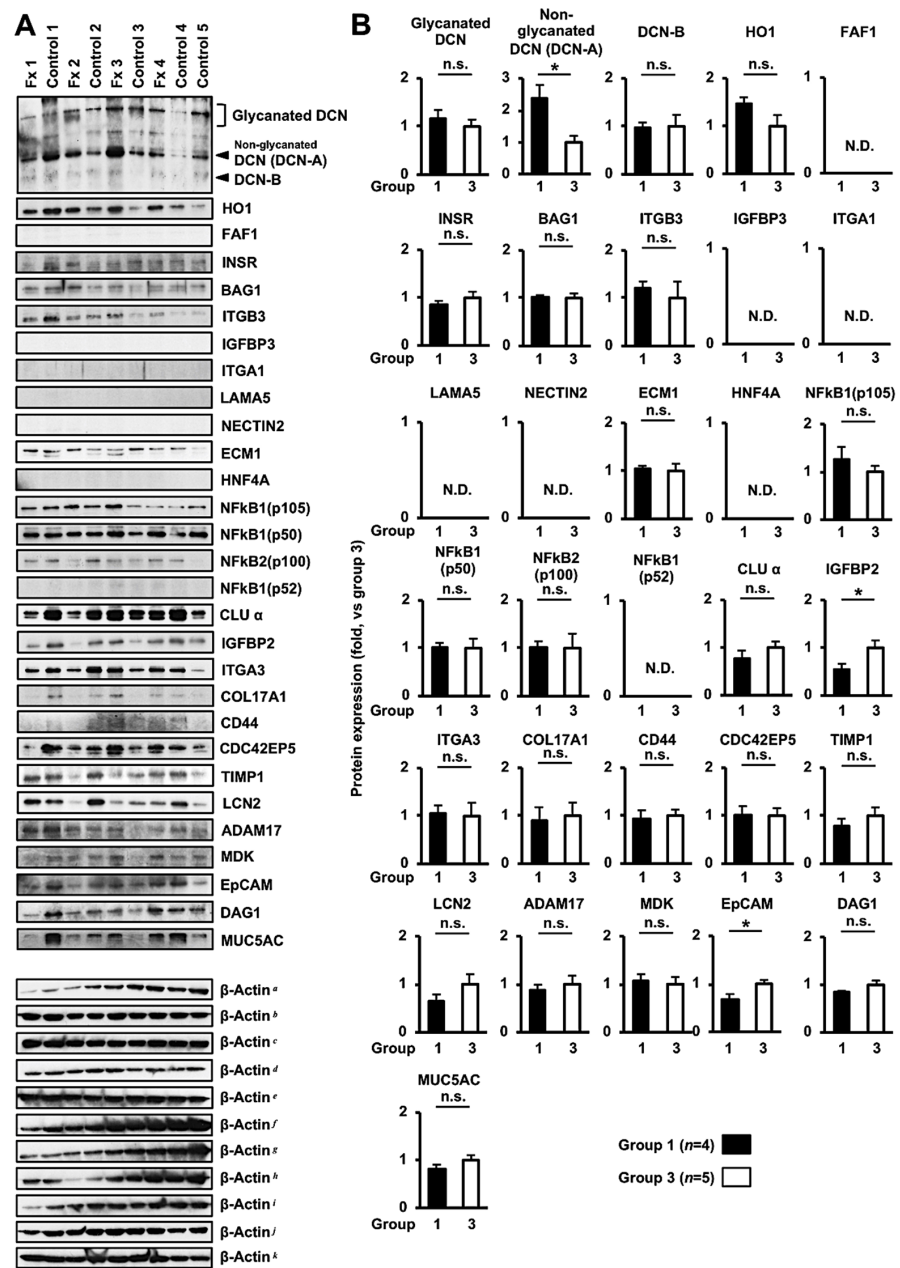


Figure 2. Protein expression profiles of tumors from patient-derived pancreatic cancer tissue-transplanted xenograft (PC-PDX) mice following fucoxanthin (Fx) administration. Protein expression levels in the tumors of Fx-high diet-administered (Group 1) and control (Group 3) mice were assessed using western blot analysis. **(A)** Each protein band for tumors of Groups 1 (Fx-high diet administered mice) and 3 (control mice). **(B)** The protein levels in tumors of PC-PDX mice in Groups 1 and 3 were normalized to that of the β -actin. Each protein level in Group 1 (black bar) was estimated against the average value (1.0-fold) of Group 3 (white bar). Data are presented as mean \pm standard error (SE) ($n = 4-5$). After the normality distribution of the results was checked using the Shapiro–Wilk test, the comparison between Groups 1 and 3 were performed using post hoc Student’s *t*-test, except for in case of EpCAM and NF κ B1 p50, which were assessed using Mann–Whitney U-test. * $p < 0.05$. n.s., no significance; and N.D., not detected. β -Actin as a loading control for membranes analyzing ^a glycanated DCN, non-glycanated DCN (DCN-A), and DCN-B, ^b ITGB3, LAMA5, and ECM1; ^c BAG1 and ITGA1; ^d HNF4A, IGFBP2, NF κ B(p105), NF κ B(p50), and COL17A1; ^e CLU α , ITGA3, NF κ B(p100), NF κ B(p52), and LCN2; ^f MDK, EpCAM, MUC5AC, and DAG1; ^g TIMP1, FAF1, and HO1; ^h IGFBP3 and CD44; ⁱ NECTIN2 and ADAM17; ^j INSR; and ^k CDC42EP5.

Subsequently, alterations in the central 26 molecules belonging to 11 upstream and downstream signals closely related to all DCN, HO1, IGFBP2, EpCAM, and LCN2 were examined in the whole tumor tissue of a PC-PDX mice, following Fx-high diet administration (Figure 3). Fx administration in group 1 significantly increased the expression of phospho(p) protein kinase B (pAKT)(Thr³⁰⁸) (1.8-fold), phospho signal transducer and activator of transcription (pSTAT3)(Ser⁷²⁷) (2.3-fold), and pSmad2(Ser^{465/467}) (2.2-fold); and tended to increase levels of phospho focal adhesion kinase (pFAK)(Tyr³⁹⁷) (1.6-fold), pPaxillin(Tyr³¹) (1.4-fold), pAKT(Ser⁴⁷³) (1.3-fold), transforming growth factor (TGF)- β 1(1.6-fold), p-p38(Thr¹⁸⁰/Tyr¹⁸²) (1.6-fold), phospho c-Jun N-terminal kinase (pJNK)(Thr¹⁸³/Tyr¹⁸⁵) (1.8-fold), and Cyclin D1 (1.5-fold), as compared to those in Group 3. The expression or activation of the other 16 proteins was minimally altered between Groups 1 and 3 or was not detected in both the groups (Figure 3).

3.5. Altered Protein Expression or Activation in FxOH-Treated Human PC Cells

Since FxOH is the prime metabolite derived from dietary Fx in the plasma and various organs of humans and mice [21,22], we have investigated the growth inhibition effects and molecular mechanisms of FxOH in human PC cells, and not Fx. Based on the gene and protein alterations induced by Fx administration in the whole tumor tissue of PC-PDX mice, we also examined the effect of FxOH on protein expression and activation in two representative human pancreatic cancer cell lines, PANC-1 and BxPC-3. We first confirmed the inhibitory effects of FxOH on the growth of PANC-1 and BxPC-3 cells. Treatment with FxOH (5 and 20 μ M) induced marked morphological changes, ranging from an elongated cell type to a round type. Additionally, FxOH showed significantly suppressed cell proliferation, in a dose-dependent manner, as determined using the cell count assay with DAPI-stained nuclei (Figure 4A,B). The percentages of cell proliferation (control 100%) were as follows: 5 μ M FxOH, 52.1 \pm 3.2%; 20 μ M FxOH, 46.1 \pm 3.4% in PANC-1 cells; 5 μ M FxOH, 59.6 \pm 3.5%; 20 μ M FxOH, 40.6 \pm 2.6% in BxPC-3 cells (Figure 4B). Next, we confirmed the effects of FxOH in PANC-1 and BxPC-3 cells with respect to molecules and signals altered in the whole tumor tissue of PC-PDX mice following Fx administration. Consequently, FxOH treatment (5 and/or 20 μ M) upregulated expression levels (\geq 1.5-fold change) of glycanated DCN, non-glycanated DCN (DCN-A), HO1, LCN2, pAKT(Ser⁴⁷³), pJNK(Thr¹⁸³/Tyr¹⁸⁵), and active forms of caspase-3, while it downregulated the expression levels (\leq 0.6-fold change) of integrin α 5, pPaxillin(Tyr³¹), and Cyclin D1 in PANC-1 cells. In addition, FxOH upregulated the expression levels (\geq 1.5-fold change) of non-glycated DCN, HO1, IGFBP2, LCN2, EpCAM, pPaxillin(Tyr³¹), pAKT(Thr³⁰⁸), p-p38(Thr¹⁸⁰/Tyr¹⁸²), pJNK(Thr¹⁸³/Tyr¹⁸⁵), and active forms of caspase-3, and downregulated the expression levels (\leq 0.6-fold change) of glycanated DCN, pAKT(Ser⁴⁷³), pSTAT3(Ser⁷²⁷), pSmad2(Ser^{465/467}), and Cyclin D1 in BxPC-3 cells. DCN-B expression in either cell line, EpCAM, pFAK(Tyr³⁹⁷), and pSmad2(Ser^{465/467}) expressions in PANC-1 cells, were detected at a very low level, with or without FxOH treatments (Figure 4C).

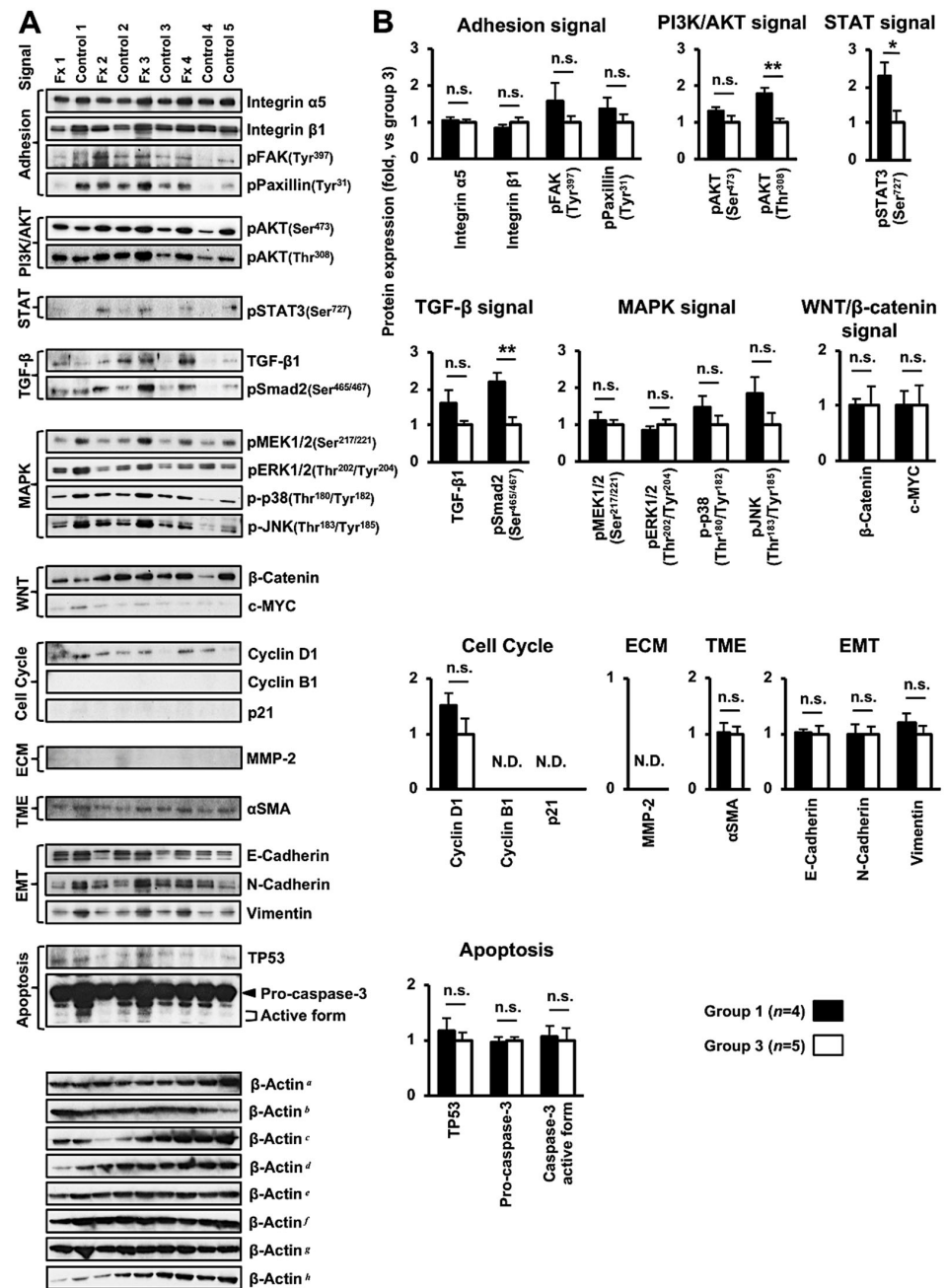


Figure 3. Protein expression and activation profiles in tumors of patient-derived pancreatic cancer tissue-transplanted xenograft (PC-PDX) mice administered fucoxanthin (Fx), considering molecules upstream and downstream of DCN, HO1, IGFBP2, EpCAM, and LCN2. Protein expression levels between the Fx-high diet-administered (Group 1) and control (Group 3) mice were measured using western blot analysis. (A) Each protein band for tumors of Groups 1 (Fx-high diet administered mice) and 3 (control mice). (B) The protein levels in tumors of PC-PDX mice in Groups 1 and 3 were normalized to that of the β -actin. The protein levels in Group 1 (black bar) were estimated against the average value (1.0-fold) in Group 3 (white bar). Data are presented as mean \pm standard error (SE) ($n = 4-5$). After the normality distribution of the results was checked using Shapiro–Wilk test, comparisons between Groups 1 and 3 were performed using post hoc Student’s *t*-test. * $p < 0.05$; ** $p < 0.01$; n.s., no significance; N.D., not detected. Fx1–4, four tumors in the Fx-high diet-administered mice (Group 1); Control 1–5, five tumors in the control mice (Group 3). β -Actin levels, as a loading control, in membranes analyzing ^a integrin $\alpha 5$, pPaxillin(Tyr³¹), E-cadherin, vimentin, and pMEK1/2(Ser^{217/221}); ^b integrin $\beta 1$, pERK1/2(Thr²⁰²/Tyr²⁰⁴), β -catenin, N-cadherin,

and cyclin D1; ^c pFAK(Tyr³⁹⁷) and pAKT(Thr³⁰⁸); ^d pAKT(Ser⁴⁷³) and pSTAT3(Ser⁷²⁷); ^e TGF-β1, pSmad2(Ser^{465/467}), MMP-2, p21, and αSMA; ^f c-MYC, TP53, pro-caspase-3 and active form of caspase-3; ^g cyclin B1; ^h p-p38(Thr¹⁸⁰/Tyr¹⁸²), and pJNK(Thr¹⁸³/Tyr¹⁸⁵). PI3K/AKT, phosphatidylinositol-3 kinase/protein kinase B; STAT, signal transducer and activator transcription; TGF-β, transforming growth factor-β; MAPK, mitogen-activated protein kinase. WNT, Wingless signal; ECM, extracellular matrix; TME, tumor microenvironment; EMT, epithelial mesenchymal transition.

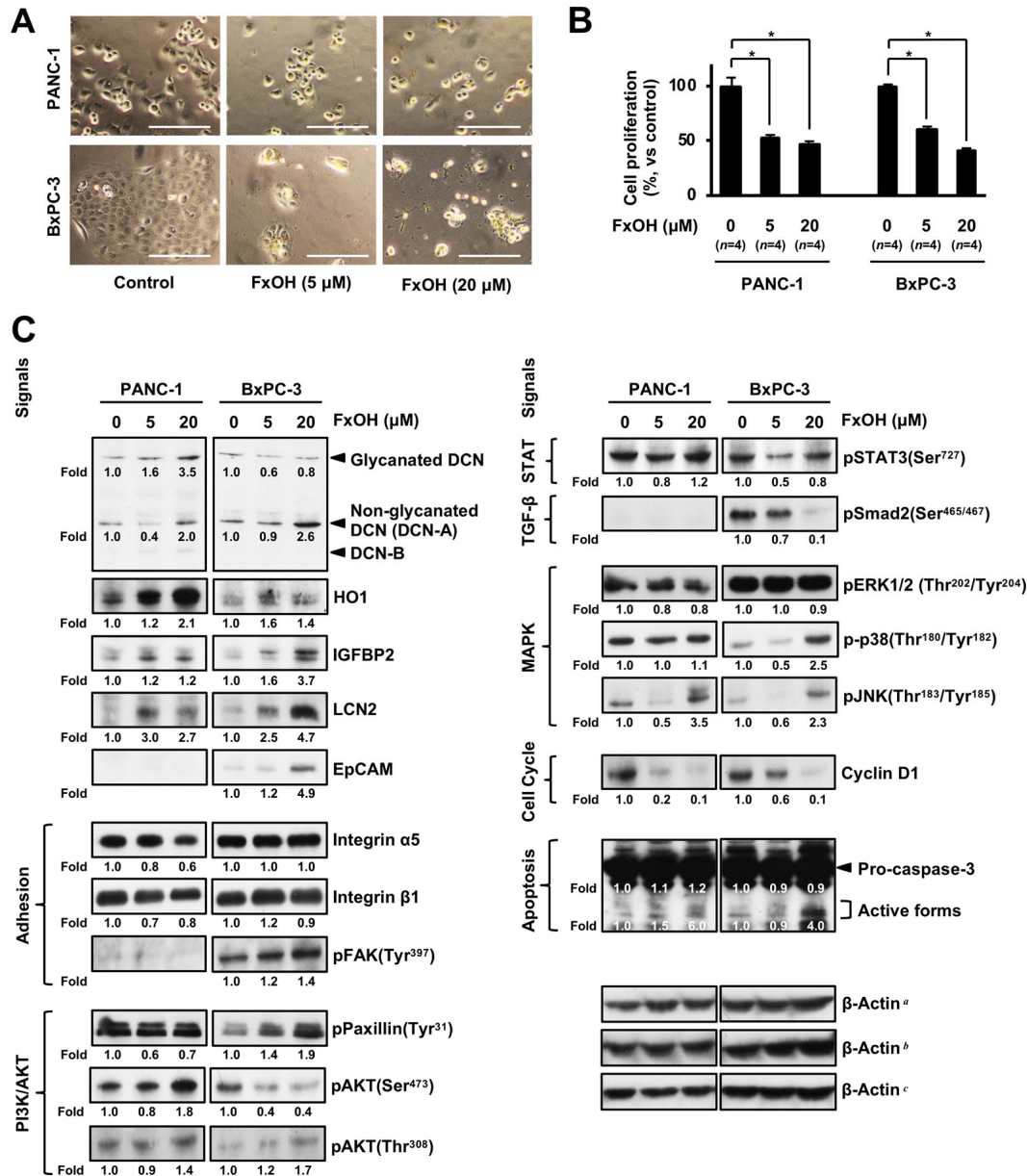


Figure 4. Growth inhibition and protein expression levels in PANC-1 and BxPC-3 cells with or without fucoxanthinol (FxoH) treatment. PANC-1 and BxPC-3 cells were treated with 5 and 20 μM FxoH for 1 day. (A) Phase contrast microscopy images. Scale bar, 200 μm. (B) Cell proliferation was measured using the cell count assay based on the DAPI-stained nuclei. Data are presented as mean ± standard error (SE) (n = 4). After the normality distribution of the results was checked using the Shapiro–Wilk test, comparisons among cells with FxoH 5 and 20 μM treatments, and control cells were performed using one-way analysis of variance with post hoc Tukey test. * p < 0.05. (C) The protein levels were measured using western blotting. β-Actin was used as a loading control. The band densities for each protein in the FxoH (5 and 20 μM)-treated PANC-1 and BxPC3 cells, as well

as control cells, were normalized to that of β -actin. Each protein level in the FxOH-treated cells was evaluated against that in the control cells as 1.0-fold. Since the bands of DCN-B, EpCAM, pFAK(Tyr³⁹⁷), and pSmad2(Ser^{465/467}) in PANC-1 cells, as well as DCN-B in BxPC-3 cells, represented little expression, these protein levels were not calculated. β -Actin, as a loading control, for membranes analyzing ^a HO1, IGFBP2, integrin α 5, pPaxillin(Tyr³¹), pAKT(Ser⁴⁷³), pSmad2(Ser^{465/467}), and Cyclin D1; ^b LCN2, EpCAM, integrin β 1, pFAK(Tyr³⁹⁷), pAKT(Thr³⁰⁸), pERK1/2(Thr²⁰²/Tyr²⁰⁴), pro-caspase-3, and active form of caspase-3; ^c glycanated DCN, non-glycanated DCN (DCN-A), DCN-B, pSTAT3(Ser⁷²⁷), p-p38(Thr¹⁸⁰/Tyr¹⁸²), and pJNK(Thr¹⁸³/Tyr¹⁸⁵). All experiments were repeated twice with the same results.

4. Discussion

In the present study, assessment of the pathological and molecular characteristics of the tumors derived from a patient with PC indicated that the tissue was an aggressive malignant primary cancer with certain genetic variations. Fx administration substantially inhibited tumor development and induced differentiation in PC-PDX mice, accompanied by altered expression of multiple molecules in both epithelial and stromal tissues. To the best of our knowledge, this is the first report to suggest the anticancer effects of Fx in human-like PC tissues, similar to clinical samples, using PDX mice.

The characteristics of the primary tumor tissue (TG₀) of a patient with PC, in addition to those to the TG₃ sample, suggested that the tissue was an aggressive malignant primary cancer tissue possessing genetic alterations in *TP53*, *KRAS*, *ARID1A*, and *NOTCH2NLC* (Tables 1 and S2). Notable frequencies of *TP53* (tumor suppressor gene), *KRAS* (oncogene), and *ARID1A* (tumor suppressor gene) mutations have been detected in the PC tissues of several patients. In particular, mutations in *TP53* and *KRAS* can lead to aberrations in signaling pathways such as mitogen-activated protein kinase (MAPK), phosphatidylinositol-3 kinase (PI3K)/AKT, DNA damage, and cell cycle, and contribute to the malignant progression of PanIN, followed by PC development. In addition, the loss of *ARID1A* function could be correlated with poor outcomes in PC [5,6,32–35]. There is limited information available regarding the genetic variation and function of *NOTCH2NLC* in PC; therefore, we did not focus on this gene or its mechanism of action in this study.

Herein, we administered the PC-PDX mouse model a Fx-high diet (0.3% Fx) ad libitum for 27 days. In Group 1, the average Fx intake from the Fx diet was 491.8 mg Fx/kg bw. The human equivalent dose based on the human body surface area was estimated as 2399.0 mg Fx/60 kg bw/human/day (491.8/12.3 \times 60), according to a previous study [36,37]. Previous toxicological studies have suggested that oral administration of 20–2,000 mg Fx/kg/bw can be deemed safe, as it does not induce any serious adverse effects in vivo [16,17]. Thus, we speculated that the Fx dose (491.8 mg Fx/kg bw/mouse/day) was within the safety range for PDX mice. However, data on the clinical safety of Fx in humans are scarce. Oral administration of Fx-rich algal extracts (1.0–8.0 mg Fx/human/day for 1–4 months) has been shown to exert anti-obesity and anti-diabetes effects in humans without serious adverse effects [18–20]. Thus, there is a need for further investigations to determine the safe dose of Fx in humans.

Administration of the Fx-high diet significantly inhibited the estimated tumor size in Group 1 (0.4-fold compared with Group 3) and strongly induced differentiation in the ADC, as compared to that in Group 3 (Figure 1B and Supplementary Table S3). Subsequently, we aimed to elucidate the molecular mechanisms underlying the anticancer and differentiation-inducing effects of Fx on tumors, focusing particularly on the proteome profiles (Supplementary Tables S4 and S5). There was enhanced expression of DCN-A (2.4-fold), HO1 (1.5-fold), p-p38(Thr¹⁸⁰/Tyr¹⁸²) (1.5-fold), and pJNK(Thr¹⁸³/Tyr¹⁸⁵) (1.8-fold), and reduced expression of IGFBP2 (0.6-fold), LCN2 (0.6-fold), and EpCAM (0.7-fold) in the tumor tissues of the Fx high diet-administered PC-PDX mice, as compared to those in the control mice (Figures 2 and 3). The in vitro experiments showed that in the expression patterns of DCN-A, HO1, p-p38(Thr¹⁸⁰/Tyr¹⁸²), and pJNK(Thr¹⁸³/Tyr¹⁸⁵) in the FxOH-treated PANC-1 and BxPC-3 cells were consistent with the Fx-administered mice (Figure 4).

DCN, a typical small leucine-rich protein, is a secreted proteoglycan embedded in the extracellular matrix (ECM). It is widely distributed as two types of DCNs in mammalian cells: an approximately 40 kDa core protein (non-glycanated DCN, or DCN-A) and an approximately 80–90 kDa glycosaminoglycan (GAG)-added type (glycanated DCN). The GAG chain in the molecule comprises variable GAGs, such as chondroitin and dermatan sulfate, and controls the distance between collagen fibrils in the ECM. DCN is a multifunctional proteoglycan that suppresses tumor growth, angiogenesis, cell cycle, inflammation, metastasis, and epithelial-mesenchymal transition (EMT) and promotes mitophagy, apoptosis, and autophagy by regulating several signals, including mesenchymal-epithelial transition factor (Met), epidermal growth factor receptor (EGFR), vascular endothelial growth factor receptor 2 (VEGFR2), WNT, MAPK, PI3K/AKT/mammalian target of rapamycin (mTOR), and TGF- β [38,39]. Furthermore, DCN is secreted by stromal cells, such as cancer-associated fibroblasts (CAFs), which can enhance the tumor microenvironment (TME) formation via the DCN paracrine effect [40]. Moreover, Zhang et al. have demonstrated that DCN-A is expressed at higher levels in paracancerous tissues than in cancerous tissues, among human PC samples, while a low molecular weight DCN (DCN-B, approximately 25 kDa) is elevated in cancerous tissues. In addition, DCN-A overexpression suppresses cell proliferation and migration and augments apoptosis-related gene expression in BxPC-3 cells, in contrast to the effects of DCN-B overexpression [41]. HO1, an inducible cytoprotective enzyme against oxidative stress, facilitates tumor microenvironment (TME) formation, chemoresistance, and anti-apoptotic action in PC cells and mouse models [42–44]. Insulin growth factor (IGF) and receptor signaling (e.g., IGF-1R) are the key pathways involved in PC development. IGF-binding proteins (IGFBPs) bind to IGFs, stabilize cytokines, and alter various downstream signals. IGFBP2 is one of six IGFBP members (IGFBP1–6) with binding sites for IGF-I, heparin, ECM, cell surface proteoglycans, and integrins in its protein sequence. It has been suggested that IGFBP2 could promote tumorigenesis, EMT, cell proliferation, invasion, metastasis, and angiogenesis through the activation of integrin, EGFR, PI3K/AKT, NF κ B, STAT3, VEGF, extracellular signal-regulated kinase (ERK), and WNT, and the suppression of p21 [45,46]. High serum levels of IGFBP2 are associated with poor survival in patients with PC [46]. LCN2, a novel adipokine, also called neutrophil gelatinase-associated lipocalin, is highly expressed in patients with PC and is a key regulator of inflammation, fibrosis, PanIN formation, survival, pancreatic tumor growth, TME, metastasis, angiogenesis, and EMT, along with the activation of NF- κ B, EGFR, and MEK/ERK expression [47,48]. EpCAM is a pan-epithelial differentiation antigen expressed in epithelial tissues that positively regulates tumorigenesis, cell proliferation, differentiation, migration, metastasis, EMT, tumor immunity, drug resistance, NF κ B, interleukins (IL-6 and IL-8), PI3K/AKT/mTOR, WNT, hepatocyte growth factor/c-Met, RAS/MAPK, and integrins [49]. p38 and JNK belong to the MAPK family and have dual functions that induce cell survival or death through various stimuli; however, their activation under severe oxidative stress (pro-oxidant effect) induces apoptosis in cancer cells [50].

Currently, there is limited evidence on the association between carotenoids and DCN in cancer. This study is the first to report an association between the anticancer effects of carotenoids and DCN expression in PDX mice and their apoptotic effects in human PC cells (Figures 2 and 4C). In addition, the expression of α smooth muscle actin (α SMA), a cancer-associated fibroblast marker protein, differed minimally between Groups 1 and 3 (Figure 3). Therefore, we speculated that DCN secreted from stromal cells contributes minimally to the anticancer effects of Fx. In addition, the DCN-B protein levels did not significantly differ between Groups 1 and 3 (Figure 2). This molecule was poorly identified in the FxOH-treated human PC cells (Figure 4C). Among all the DCN types, only DCN-A may play an important role in the anticancer effects of Fx in mice. To date, some researchers have demonstrated the functional validations of DCN, IGFBP2, LCN2, and EpCAM in human PC cells. Treatment of DCN-expressing oncolytic adenovirus significantly suppressed the cell growth in human PC MIA PaCa-2 and PANC-1 cells and inhibited pancreatic tumorigenesis in athymic nude mice with orthotopic transplantation of MIA PaCa-2 [51].

IGFBP-2 gene knockdown attenuated migration, invasion, and EMT in human PC BxPC-3 and CFPAC cells [52]. LCN2 gene knockdown inhibited cell attachment and invasion in human PC BxPC-3 and HPAF-II cells [53]. An intraperitoneal administration of a bispecific antibody (EpCAM and CD3) suppressed a tumor growth in xenograft mice transplanted of BxPC-3 cells [54]. Thus, DCN, IGFBP2, LCN2, and EpCAM are effective molecules for the growth inhibition in human PC cells. Several carotenoids are responsible for regulating oxidative stress in normal cells through their antioxidant activities. Accumulating evidence has demonstrated that certain carotenoids containing Fx, astaxanthin, bixin, β -carotene, β -cryptoxanthin, lutein, and lycopene can exert the pro-oxidant actions against various cancer cells, inducing high levels of intracellular reactive oxygen species (ROS). ROS-mediated apoptosis enhances DNA damage and expression of pATR, pATM, p-p38, pJNK, Bax, p53, caspases, p21, p27, and heat-shock proteins (HSPs), and reduced levels of pAKT, Bcl-2, and pERK expression [55]. Intracellular levels of ROS, including the superoxide radical/anion, hydroxyl radical, and hydrogen peroxide, are modulated by antioxidant enzymes such as superoxide dismutase, glutathione (GSH) peroxidase, GSH reductase, and catalase. In the present study, tumor tissues from Fx-treated PC-PDX mice showed the upregulated trends for HO1, p-p38 (Thr¹⁸⁰/Tyr¹⁸²), and pJNK (Thr¹⁸³/Tyr¹⁸⁵) (Figures 2 and 3). Furthermore, upregulated expression of HO1, p-p38(Thr¹⁸⁰/Tyr¹⁸²), and/or pJNK(Thr¹⁸³/Tyr¹⁸⁵) was observed during apoptosis induction in FxOH-treated PANC-1 and BxPC-3 cells (Figure 4C). The in vitro and in vivo experiments suggest that although HO1 upregulation would result from oxidative stress, the pro-oxidant effects mediated through p38 and JNK activation may trigger suppressive effects on tumor growth in Fx-administered PC-PDX mice.

On the other hand, the expressions of IGFBP2, EpCAM, and LCN2 showed the opposite patterns between in vivo and in vitro experiments (Figures 2 and 3, and Figure 4C). The differences in its molecular expression in cells and animal tissues may depend on the property of cancer cells prior to compound addition or on the interaction with stromal cell populations. In addition, some of molecular alteration patterns of in vitro and in vivo experiments in the present study were different from those of our previous studies: FxOH-treated mouse PDAC cell line (KMPC44) established from the *Ptfl1a^{Cre/+}; LSL-K-ras^{G12D/+}* mice and a hamster PDAC cell line (HaPC-5) established from the BOP-treated Syrian golden hamster, and Fx-administered PC mouse (C57BL/6J) model with allogenic and orthotopic transplantations of the KMPC44 cells (27–29). Moreover, functional modifications of cellular signals are frequently associated with drug resistance and cancer cell survival. The activation of PI3K/AKT, integrins/FAK, TGF- β , IGF1R, EMT, and nuclear factor erythroid 2 p45-related factor 2/HO1 was found to exert key roles in compensating for cell resistance and survival against anticancer drug exposure [56,57]. The upregulated expression (≥ 1.5 -fold change) of HO1, pFAK(Tyr³⁹⁷), pAKT(Thr³⁰⁸), pSTAT3(Ser⁷²⁷), TGF- β 1, pSmad2(Ser^{465/467}), and Cyclin D1 in the tumor tissue of Fx-treated PC-PDX mice might be a partial compensatory mechanism for survival and chemoresistance (Figures 2 and 3). Similarly, the upregulated expression (≥ 1.5 -fold change) of HO1, IGFBP2, LCN2, EpCAM, pPaxillin (Tyr³¹), pAKT (Ser⁴⁷³), and pAKT (Thr³⁰⁸) in FxOH-treated PC cells may be a partial compensatory mechanism in cancer cell models (Figure 4C). For future application of Fx as an anticancer drug for individual patients with PC, it is necessary to elucidate the anticancer mechanisms of Fx (or FxOH) at any treating method using various animal and cell models, such as PDX, three-dimensional cell culture models recapitulating the clonal heterogeneity, and two-dimensional co-culture models in tumor and stromal cells [10,11].

TG₃ tumor samples showed genetic alterations in *TP53*, *KRAS*, and *ARID1A* expression levels. The presence of *KRAS* mutations in patients is correlated with low *DCN* gene expression [58]. In addition, the combined delivery of *KRAS* and *IGFBP2* induced astrocytoma development in vivo [59]. *LCN2* reportedly contributes to PanIN formation and poor survival in a transgenic *K-ras^{G12D}* PC mouse model [44]. *Kras^{G12D}* and loss of *Arid1a* function concomitantly induce PanIN development in a PC mouse model [60]. Fx may have restraining effects on *KRAS* and *ARID1A* mutation-triggered pancreatic dysfunction.

A TG₅ (corresponding to F₅) sample was used in this study. Generally, the third generation (TG₃/F₃) in PDX mice is used for anticancer drug efficacy. As consecutive passages of human tumors engrafted into PDX mice cause gradual histological, stromal, and genetic shifts, the progression of tumor generation is a risk factor for altering the effect of the anticancer drugs. Tentler et al. have revealed that the gene expression profiles of F₅/F₀ in PDX mice were more diverse than those of F₃/F₀ [61]. However, the tumor sample donated by the J-PDX library was already TG₃. Thus, we proceeded with the understanding that these limitations may have hindered the findings of this study.

5. Conclusions

Figure 5 summarizes the molecular alterations underlying the effects of Fx in a PC-PDX mouse model. Based on our findings, Fx administration considerably abrogated tumor development and induced tumor differentiation in a PC-PDX mouse model, along with comprehensive alterations in 1205 proteins in proteome analysis. Considering these molecular alterations, Fx-administered PC-PDX mice showed increased expression of non-glycanated DCN (DCN-A), p-p38(Thr¹⁸⁰/Tyr¹⁸²), and pJNK(Thr¹⁸³/Tyr¹⁸⁵), as well as decreased expression of IGFBP2, EpCAM, and LCN2. Our results suggest that the increase in DCN and pro-oxidant signals and the inhibition of IGFBP2-, EpCAM-, and LCN2-related signals are key regulators of tumor suppression in PC-PDX mice. Therefore, Fx could serve as a promising candidate for cancer therapy in patients with PC, and there is a need for further investigations using other PC-PDX models to confirm the anticancer effects of Fx.

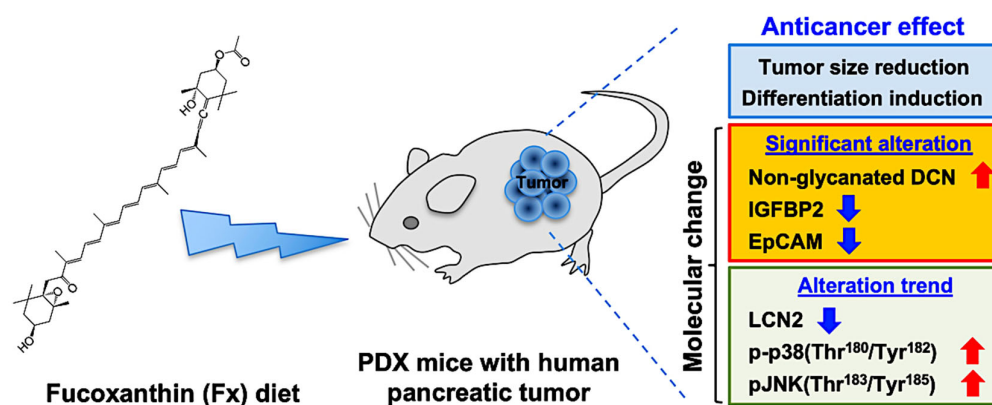


Figure 5. Possible mechanisms underlying the anticancer and differentiation effects of fucoxanthin (Fx) against a patient derived xenograft (PDX) mice with a human pancreatic cancer. Non-glycanated DCN, non-glycanated decorin (DCN-A); IGFBP2, insulin growth factor binding protein 2; EpCAM, epithelial cell adhesion molecule; LCN2, lipocalin 2; p-p38(Thr¹⁸⁰/Tyr¹⁸²), phosphorylated p38(Thr¹⁸⁰/Tyr¹⁸²); pJNK(Thr¹⁸⁰/Tyr¹⁸²), phosphorylated c-Jun N-terminal kinase(Thr¹⁸³/Tyr¹⁸⁵). Red and blue arrows show upregulated (activated) and downregulated proteins.

Supplementary Materials: The following supporting information can be downloaded at: <https://www.mdpi.com/article/10.3390/onco3040016/s1>, Figure S1: A highly polar marine xanthophyll of fucoxanthin; Figure S2: Representative histopathology of pancreatic adenocarcinoma (ADC); Table S1: Supporting information of each antibody; Table S2: Profile of four amino acid substitution polymorphisms in a pancreatic adenocarcinoma of a patient; Table S3: Incidence (%) of different differentiated adenocarcinoma (ADC) in patient-derived pancreatic cancer tissue-transplanted xenograft (PC-PDX) mice administered fucoxanthin (Fx); Table S4: Profile of upregulated proteins identified by LC-MS/MS in whole tumor tissue of patient-derived pancreatic cancer tissue-transplanted xenograft (PC-PDX) mice administered fucoxanthin (Fx); Table S5: Profile of downregulated proteins identified by LC-MS/MS in whole tumor tissue of patient-derived pancreatic cancer tissue-transplanted xenograft (PC-PDX) mice administered fucoxanthin (Fx).

Author Contributions: M.T. (Masaru Terasaki) conceived and designed the study. M.T. (Masaru Terasaki), S.S., T.T., H.M., M.S., T.O., Y.S., S.H., C.M. and M.T. (Mami Takahashi) performed the experiments. M.T. (Masaru Terasaki) wrote the manuscript. K.M., Y.K., J.H., S.Y. and A.H. performed data interpretation, reviewed intellectual content of the work and edited the manuscript. All the listed authors have read and approved the final manuscript and agree to be responsible for all aspects of the research to ensure that the accuracy or integrity of any part of the work is appropriately investigated and resolved. All authors have read and agreed to the published version of the manuscript.

Funding: This work was supported in part by the Japan Society for the Promotion of Science, KAKENHI (grant no. 20K05879). The National Cancer Center J-PDX library was partly supported by AMED (grant no. 17 pc0101011h0001) and the National Cancer Center Research and Development Fund of Japan.

Institutional Review Board Statement: This study was conducted according to the Guidelines of the Declaration of Helsinki and approved by the Institutional Review Board of the National Cancer Center Research Institute, considering the informed consent, sample collection, use of patient data transmitted in the study (identification code, 2015-123 and 2021-163; authorization, 2015 and 2021), and the establishment of the PDX tumor (identification codes, T17-020, T17-073 and T19-008; authorization, 2017 and 2021). The Institutional Review Boards of the National Cancer Center Research Institute (identification code, 2021-163; authorization, 2021) and the Health Sciences University of Hokkaido approved the animal experiments in PDX mice using Fx (identification code, 21P003; authorization, 2021).

Informed Consent Statement: Informed consent was obtained from all patients involved in the establishment of the J-PDX library at the National Cancer Center.

Data Availability Statement: The data used in this study are available from the corresponding author upon reasonable request.

Acknowledgments: Fx-oil (product name, Fucoxanthin-5KW[®]) and the control oil were kindly supplied by Oryza Oil & Fat Chemical Co., Ltd. (Ichinomiya City, Aichi, Japan). We would like to thank the laboratory students, Wataru Murase, Ayaka Yasuda, Momoka Wagatsuma, Takumi Ouchi, Yoshiro Kikuchi, and Yuichi Shimazaki, and Atsuhito Kubota of the School of Pharmaceutical Sciences, and the staff of the Center for Experimental Animals at the Health Sciences University of Hokkaido for their support with animal treatment. We thank the patients and staff who contributed to the establishment of the National Cancer Center J-PDX Library.

Conflicts of Interest: The authors declare no conflict of interest, except for Masaru Terasaki. Masaru Terasaki is listed as the inventor of a Japanese patent application for the anticancer effects of Fx-oil (Oryza Oil & Fat Chemical Co., Ltd., Ichinomiya City, Aichi, Japan) in PDX mice. The data used in this study are partially described in the submitted patent applications section. However, Masaru Terasaki did not receive royalties from Oryza Oil and Fat Chemical Co., Ltd.

References

1. Sung, H.; Ferlay, J.; Siegel, R.L.; Laversanne, M.; Soerjomataram, I.; Jemal, A.; Bray, F. Global Cancer Statistics 2020: GLOBOCAN Estimates of Incidence and Mortality Worldwide for 36 Cancers in 185 Countries. *CA Cancer J. Clin.* **2021**, *71*, 209–249. [CrossRef]
2. Rahib, L.; Wehner, M.R.; Matrisian, L.M.; Nead, K.T. Estimated Projection of US Cancer Incidence and Death to 2040. *JAMA N. Open* **2021**, *4*, e214708. [CrossRef]
3. American Cancer Society. Pancreatic Cancer, American Cancer Society: Atlanta, GA, USA, 2021. Available online: <https://www.cancer.org/cancer/pancreatic-cancer.html> (accessed on 18 March 2023).
4. World Cancer Research Fund; American Institute for Cancer Research. Diet, Nutrition, Physical Activity and Pancreatic Cancer 2012. Revised 2018. Available online: <https://www.wcrf.org> (accessed on 18 March 2023).
5. Pelosi, E.; Castelli, G.; Testa, U. Pancreatic Cancer: Molecular Characterization, Clonal Evolution and Cancer Stem Cells. *Biomedicines* **2017**, *5*, 65. [CrossRef]
6. Cicenias, J.; Kvederaviciute, K.; Meskinyte, I.; Meskinyte-Kausiliene, E.; Skeberdyte, A.; Cicenias, J. KRAS, TP53, CDKN2A, SMAD4, BRCA1, and BRCA2 Mutations in Pancreatic Cancer. *Cancers* **2017**, *9*, 42. [CrossRef]
7. Hingorani, S.R.; Petricoin, E.F.; Maitra, A.; Rajapakse, V.; King, C.; Jacobetz, M.A.; Ross, S.; Conrads, T.P.; Veenstra, T.D.; Hitt, B.A.; et al. Preinvasive and Invasive Ductal Pancreatic Cancer and Its Early Detection in The Mouse. *Cancer Cell* **2003**, *4*, 437–450. [CrossRef]

8. Ijichi, H.; Chytil, A.; Gorska, E.; Aakre, M.E.; Fujitani, Y.; Fujitani, S.; Wright, C.V.E.; Moses, H.L. Aggressive Pancreatic Ductal Adenocarcinoma in Mice Caused by Pancreas-specific Blockade of Transforming Growth Factor-beta Signaling in Cooperation with Active Kras Expression. *Genes Dev.* **2006**, *20*, 3147–3160. [[CrossRef](#)]
9. Hingorani, S.R.; Wang, L.; Multani, A.S.; Combs, C.; Deramaudt, T.B.; Hruban, R.H.; Rustgi, A.K.; Chang, S.; Tuveson, D.A. *Trp53^{R172H}* and *Kras^{G12D}* Cooperate to Promote Chromosomal Instability and Widely Metastatic Pancreatic Ductal Adenocarcinoma in Mice. *Cancer Cell* **2005**, *7*, 469–483. [[CrossRef](#)]
10. Takahashi, M.; Hori, M.; Mutoh, M.; Wakabayashi, K.; Nakagama, H. Experimental Animal Models of Pancreatic Carcinogenesis for Prevention Studies and Their Relevance to Human Disease. *Cancers* **2011**, *3*, 582–602. [[CrossRef](#)]
11. Hou, X.; Du, C.; Lu, L.; Yuan, S.; Zhan, M.; You, P.; Du, H. Opportunities and Challenges of Patient-derived Models in Cancer Research: Patient-derived Xenografts, Patient-derived Organoid and Patient-derived Cells. *World J. Surg. Oncol.* **2022**, *20*, 37. [[CrossRef](#)]
12. Pan, B.; Wei, X.; Xu, X. Patient-derived Xenograft Models in Hepatopancreatobiliary Cancer. *Cancer Cell Int.* **2022**, *22*, 41. [[CrossRef](#)]
13. Izumchenko, E.; Meir, J.; Bedi, A.; Wysocki, P.T.; Hoque, M.O.; Sidransky, D. Patient-derived Xenografts as Tools in Pharmaceutical Development. *Clin. Pharmacol. Ther.* **2016**, *99*, 612–621. [[CrossRef](#)] [[PubMed](#)]
14. Zhang, F.; Wang, W.; Long, Y.; Liu, H.; Cheng, J.; Guo, L.; Li, R.; Meng, C.; Yu, S.; Zhao, Q.; et al. Characterization of Drug Responses of Mini Patient-derived Xenografts in Mice for Predicting Cancer Patient Clinical Therapeutic Response. *Cancer Commun.* **2018**, *38*, 60. [[CrossRef](#)]
15. Tavares, R.S.N.; Maria-Engler, S.S.; Colepiccolo, P.; Debonis, H.M.; Schäfer-Korting, M.; Marx, U.; Gaspar, L.R.; Zoschke, C. Skin Irritation Testing Beyond Tissue Viability: Fucoxanthin Effects on Inflammation, Homeostasis, and Metabolism. *Pharmaceutics* **2020**, *12*, 136. [[CrossRef](#)] [[PubMed](#)]
16. Beppu, F.; Niwano, Y.; Tsukui, T.; Hosokawa, M.; Miyashita, K. Single and Repeated Oral Dose Toxicity Study of Fucoxanthin (FX), A Marine Carotenoid, in Mice. *J. Toxicol. Sci.* **2009**, *34*, 501–510. [[CrossRef](#)] [[PubMed](#)]
17. Iio, K.; Okada, Y.; Ishikura, M. Single and 13-week Oral Toxicity Study of Fucoxanthin Oil from Microalgae in Rats. *Sokuhin Eiseigaku Zasshi* **2011**, *52*, 183–189. [[CrossRef](#)]
18. Hitoe, S.; Shimoda, H. Seaweed Fucoxanthin Supplementation Improves Obesity Parameters in Mild Obese Japanese Subjects. *Funct. Foods Health Dis.* **2017**, *7*, 246–262. [[CrossRef](#)]
19. Mikami, N.; Hosokawa, M.; Miyashita, K.; Sohma, H.; Ito, Y.M.; Kokai, Y. Reduction of HbA1c Levels by Fucoxanthin-enriched Akamoku Oil Possibly Involves the Thrifty Allele of Uncoupling Protein 1 (UCP1): A Randomised Controlled Trial in Normal-Weight and Obese Japanese Adults. *J. Nutr. Sci.* **2017**, *6*, e5. [[CrossRef](#)]
20. Adibov, M.; Ramazanov, Z.; Seifulla, R.; Grachev, S. The Effects of Xanthigen in The Weight Management of Obese Premenopausal Women with Non-alcoholic Fatty Liver Disease and Normal Liver Fat. *Diabetes Obes. Metab.* **2010**, *12*, 72–81. [[CrossRef](#)]
21. Hashimoto, T.; Ozaki, Y.; Mizuno, M.; Yoshida, M.; Nishitani, Y.; Azuma, T.; Komoto, A.; Maoka, T.; Tanino, Y.; Kanazawa, K. Pharmacokinetics of Fucoxanthinol in Human Plasma after the Oral Administration of Kombu Extract. *Br. J. Nutr.* **2012**, *107*, 1566–1569. [[CrossRef](#)]
22. Yonekura, L.; Kobayashi, M.; Terasaki, M.; Nagao, A. Keto-carotenoids Are the Major Metabolites of Dietary Lutein and Fucoxanthin in Mouse Tissues. *J. Nutr.* **2010**, *140*, 1824–1831. [[CrossRef](#)]
23. Terasaki, M.; Kubota, A.; Kojima, H.; Maeda, H.; Miyashita, K.; Kawagoe, C.; Mutoh, M.; Tanaka, T. Fucoxanthin and Colorectal Cancer Prevention. *Cancers* **2021**, *13*, 2379. [[CrossRef](#)] [[PubMed](#)]
24. Nishino, H.; Murakoshi, M.; Tokuda, H.; Satomi, Y. Cancer Prevention by Carotenoids. *Arch. Biochem. Biophys.* **2009**, *483*, 165–168. [[CrossRef](#)] [[PubMed](#)]
25. Mei, C.; Zhou, S.; Zhu, L.; Ming, J.; Zeng, F.; Xu, R. Antitumor Effects of Laminaria Extract Fucoxanthin on Lung Cancer. *Mar. Drugs* **2017**, *15*, 39. [[CrossRef](#)] [[PubMed](#)]
26. Yasuda, A.; Wagatsuma, M.; Murase, W.; Kubota, A.; Kojima, H.; Ohta, T.; Hamada, J.; Maeda, H.; Terasaki, M. Fucoxanthinol Promotes Apoptosis in MCF-7 and MDA-MB-231 Cells by Attenuating Laminins-Integrins Axis. *Onco* **2022**, *2*, 145–163. [[CrossRef](#)]
27. Terasaki, M.; Inoue, T.; Murase, W.; Kubota, A.; Kojima, H.; Kojoma, M.; Ohta, T.; Maeda, H.; Miyashita, K.; Mutoh, M.; et al. A Fucoxanthinol Induces Apoptosis in a Pancreatic Intraepithelial Neoplasia Cell. *Cancer Genom. Proteom.* **2021**, *18*, 133–146. [[CrossRef](#)]
28. Terasaki, M.; Nishizaka, Y.; Murase, W.; Kubota, A.; Kojima, H.; Kojoma, M.; Tanaka, T.; Maeda, H.; Miyashita, K.; Mutoh, M.; et al. Effect of Fucoxanthinol on Pancreatic Ductal Adenocarcinoma Cells From An *N*-Nitrosobis(2-oxopropyl)amine-initiated Syrian Golden Hamster Pancreatic Carcinogenesis Model. *Cancer Genom. Proteom.* **2021**, *18* (Suppl. 3), 407–423. [[CrossRef](#)]
29. Murase, W.; Kamakura, Y.; Kawakami, S.; Yasuda, A.; Wagatsuma, M.; Kubota, A.; Kojima, H.; Ohta, T.; Takahashi, M.; Mutoh, M.; et al. Fucoxanthin Prevents Pancreatic Tumorigenesis in C57BL/6J Mice That Received Allogenic and Orthotopic Transplants of Cancer Cells. *Int. J. Mol. Sci.* **2021**, *22*, 13620. [[CrossRef](#)]
30. Lu, J.; Wu, X.J.; Hassouna, A.; Wang, K.S.; Li, Y.; Feng, T.; Zhao, Y.; Jin, M.; Zhang, B.; Ying, T.; et al. Gemcitabine-fucoxanthin Combination in Human Pancreatic Cancer Cells. *Biomed. Rep.* **2023**, *19*, 46. [[CrossRef](#)]
31. Yagishita, S.; Kato, K.; Takahashi, M.; Imai, T.; Yatabe, Y.; Kuwata, T.; Suzuki, M.; Ochiai, A.; Ohtsu, A.; Shimada, K.; et al. Characterization of The Large-scale Japanese Patient-derived Xenograft (J-PDX) library. *Cancer Sci.* **2021**, *112*, 2454–2466. [[CrossRef](#)]

32. The Cancer Genome Atlas Research Network. Integrated Genomic Characterization of Pancreatic Ductal Adenocarcinoma. *Cancer Cell* **2017**, *32*, 185–203. [[CrossRef](#)]
33. Waddell, N.; Pajic, M.; Patch, A.M.; Chang, D.K.; Kassahn, K.S.; Bailey, P.; Johns, A.L.; Miller, D.; Nones, K.; Quek, K.; et al. Whole Genomes Redefine the Mutational Landscape of Pancreatic Cancer. *Nature* **2015**, *518*, 495–501. [[CrossRef](#)] [[PubMed](#)]
34. Witkiewicz, A.K.; McMillan, E.A.; Balaji, U.; Baek, G.; Lin, W.C.; Mansour, J.; Mollae, M.; Wagner, K.U.; Koduru, P.; Yopp, A.; et al. Whole-exome Sequencing of Pancreatic Cancer Defines Genetic Diversity and Therapeutic Targets. *Nature Commun.* **2015**, *6*, 6744. [[CrossRef](#)] [[PubMed](#)]
35. Jones, S.; Zhang, X.; Parsons, D.W.; Lin, J.C.H.; Leary, R.J.; Angenendt, P.; Mankoo, P.; Carter, H.; Kamiyama, H.; Jimeno, A.; et al. Core Signaling Pathways in Human Pancreatic Cancers Revealed by Global Genomic Analyses. *Science* **2008**, *321*, 1801–1806. [[CrossRef](#)] [[PubMed](#)]
36. Nair, A.B.; Jacob, S. A Simple Practice Guide for Dose Conversion between Animals and Human. *J. Basic Clin. Pharm.* **2016**, *7*, 27–31. [[CrossRef](#)] [[PubMed](#)]
37. U.S. Food & Drug Administration. *Estimating the Maximum Safe Starting Dose in Initial Clinical Trials for Therapeutics in Adult Healthy Volunteers*; U.S. Food & Drug Administration: Rockville, MD, USA, 2005. Available online: <https://www.fda.gov/regulatory-information/search-fda-guidance-documents/estimating-maximum-safe-starting-dose-initial-clinical-trials-therapeutics-adult-healthy-volunteers> (accessed on 27 March 2023).
38. Diehl, V.; Huber, L.S.; Trebicka, J.; Wygrecka, M.; Lozzo, R.V.; Schaefer, L. The Role of Decorin and Biglycan Signaling in Tumorigenesis. *Front. Oncol.* **2021**, *11*, 801801. [[CrossRef](#)] [[PubMed](#)]
39. Sainio, A.O.; Järveläinen, H.T. Decorin-mediated Oncosuppression—A Potential Future Adjuvant Therapy for Human Epithelial Cancers. *Br. J. Pharmacol.* **2019**, *176*, 5–15. [[CrossRef](#)]
40. Buraschi, S.; Neill, T.; Owens, R.T.; Iniguez, L.A.; Purkins, G.; Vadigepalli, R.; Evans, B.; Schaefer, L.; Peiper, S.C.; Wang, Z.X.; et al. Decorin Protein Core Affects the Global Gene Expression Profile of the Tumor Microenvironment in a Triple-Negative Orthotopic Breast Carcinoma Xenograft Model. *PLoS ONE* **2012**, *7*, e45559. [[CrossRef](#)]
41. Zhang, L.; Liu, C.; Gao, H.; Zhou, C.; Qin, W.; Wang, J.; Meng, L.; Wang, H.; Ren, Q.; Zhang, Y. Study on the expression profile and role of decorin in the progression of pancreatic cancer. *Aging* **2021**, *13*, 14989–14998. [[CrossRef](#)]
42. Ahmad, I.M.; Dafferner, A.J.; O’Connell, K.A.; Mehla, K.; Britigan, B.E.; Hollingsworth, M.A.; Abdalla, M.Y. Heme Oxygenase-1 Inhibition Potentiates the Effects of Nab-Paclitaxel-Gemcitabine and Modulates the Tumor Microenvironment in Pancreatic Ductal Adenocarcinoma. *Cancers* **2021**, *13*, 2264. [[CrossRef](#)]
43. Kim, E.J.; Kim, Y.J.; Lee, H.I.; Jeong, S.H.; Nam, H.J.; Cho, J.H. NRF2 Knockdown Resensitizes 5-Fluorouracil-Resistant Pancreatic Cancer Cells by Suppressing HO-1 and ABCG2 Expression. *Int. J. Mol. Sci.* **2020**, *21*, 4646. [[CrossRef](#)]
44. Nuhn, P.; Künzli, B.M.; Hennig, R.; Mitkus, T.; Ramanauskas, T.; Nobiling, R.; Meuer, S.C.; Friess, H.; Berberat, P.O. Heme Oxygenase-1 and Its Metabolites Affect Pancreatic Tumor Growth In Vivo. *Mol. Cancer* **2009**, *8*, 37. [[CrossRef](#)] [[PubMed](#)]
45. Li, T.; Forbes, M.E.; Fuller, G.N.; Li, J.; Yang, X.; Zhang, W. IGFBP2: Integrative Hub of Developmental and Oncogenic Signaling Network. *Oncogene* **2020**, *39*, 2243–2257. [[CrossRef](#)] [[PubMed](#)]
46. Thomas, D.; Radhakrishnan, P. Role of Tumor and Stroma-Derived IGF/IGFBPs in Pancreatic Cancer. *Cancers* **2020**, *12*, 1228. [[CrossRef](#)] [[PubMed](#)]
47. Gumper, K.; Dangel, A.W.; Pita-Grisanti, V.; Krishna, S.G.; Lara, L.F.; Mase, T.; Papachristou, G.I.; Conwell, D.L.; Hart, P.A.; Cruz-Monserrate, Z. Lipocalin-2 Expression and Function in Pancreatic Diseases. *Pancreatology* **2020**, *20*, 419–424. [[CrossRef](#)]
48. Gomez-Chou, S.B.; Swidnicka-Siergiejko, A.K.; Badi, N.; Chavez-Tomar, M.; Lesinski, G.B.; Bekaii-Saab, T.; Farren, M.R.; Mace, T.A.; Schmidt, C.; Liu, Y.; et al. Lipocalin-2 Promotes Pancreatic Ductal Adenocarcinoma by Regulating Inflammation in the Tumor Microenvironment. *Cancer Res.* **2017**, *77*, 2647–2660. [[CrossRef](#)]
49. Barzaman, K.; Vafaei, R.; Samadi, M.; Kazemi, M.H.; Hosseinzadeh, A.; Merikhian, P.; Moradi-Kalbolandi, S.; Eisavand, M.R.; Dinvari, H.; Farahmand, L. Anti-cancer Therapeutic Strategies Based on HGF/MET, EpCAM, and Tumor-stromal Cross Talk. *Cancer Int.* **2022**, *22*, 259. [[CrossRef](#)]
50. Kciuk, M.; Gielecińska, A.; Budzinska, A.; Mojzych, M.; Kontek, R. Metastasis and MAPK Pathways. *Int. J. Mol. Sci.* **2022**, *23*, 3847. [[CrossRef](#)]
51. Li, Y.; Hong, J.W.; Oh, J.E.; Yoon, A.R.; Yun, C.O. Potent Antitumor Effect of Tumor Microenvironment-targeted Oncolytic Adenovirus Against Desmoplastic Pancreatic Cancer. *Int. J. Cancer* **2018**, *142*, 392–413. [[CrossRef](#)]
52. Liu, H.; Li, L.; Chen, H.; Kong, R.; Pan, S.; Hu, J.; Wang, Y.; Li, Y.; Sun, B. Silencing IGFBP-2 Decreases Pancreatic Cancer Metastasis and Enhances Chemotherapeutic Sensitivity. *Oncotarget* **2017**, *8*, 61674–616866. [[CrossRef](#)]
53. Leung, L.; Radulovich, N.; Zhu, C.Q.; Organ, S.; Bandarchi, B.; Pintille, M.; To, C.; Panchal, D.; Tsao, M.S. Lipocalin2 Promotes Invasion, Tumorigenicity and Gemcitabine Resistance in Pancreatic Ductal Adenocarcinoma. *PLoS ONE* **2012**, *7*, e46677. [[CrossRef](#)]
54. Salnikov, A.V.; Groth, A.; Apel, A.; Kallifatidis, G.; Beckermann, B.M.; Khamidjanov, A.; Ryschich, E.; Büchler, M.W.; Herr, I.; Moldenhauer, G. Targeting of Cancer Stem Cell Marker EpCAM by Bispecific Antibody EpCAMxCD3 Inhibits Pancreatic Carcinoma. *J. Cell Mol. Med.* **2009**, *13*, 4023–4033. [[CrossRef](#)] [[PubMed](#)]
55. Shin, J.; Song, M.H.; Oh, J.W.; Keum, Y.S.; Saini, R.K. Pro-Oxidant Actions of Carotenoids in Triggering Apoptosis of Cancer Cells: A Review of Emerging Evidence. *Antioxidants* **2020**, *9*, 532. [[CrossRef](#)] [[PubMed](#)]
56. Housman, G.; Byler, S.; Heerboth, S.; Lapinska, K.; Longacre, M.; Snyder, N.; Sarkar, S. Drug Resistance in Cancer: An Overview. *Cancers* **2014**, *6*, 1769–1792. [[CrossRef](#)] [[PubMed](#)]

57. Furfaro, A.L.; Traverso, N.; Domenicotti, C.; Piras, S.; Moretta, L.; Marinari, U.M.; Pronzato, M.A.; Nitti, M. The Nrf2/HO-1 Axis in Cancer Cell Growth and Chemoresistance. *Oxid. Med. Cell. Longev.* **2016**, *2016*, 1958174. [[CrossRef](#)] [[PubMed](#)]
58. Mlakar, V.; Berginc, G.; Volavsek, M.; Stor, Z.; Rems, M.; Glavac, D. Presence of Activating KRAS Mutations Correlates Significantly with Expression of Tumour Suppressor Genes DCN and TP53 in Colorectal Cancer. *BMC Cancer* **2009**, *9*, 282. [[CrossRef](#)] [[PubMed](#)]
59. Dunlap, S.M.; Celestino, J.; Wang, H.; Jiang, R.; Holland, E.C.; Fuller, G.N.; Zhang, W. Insulin-like growth factor binding protein 2 promotes glioma development and progression. *Proc. Natl. Acad. Sci. USA* **2007**, *104*, 11736–11741. [[CrossRef](#)]
60. Livshits, G.; Alonso-Curbelo, D.; Morris, J.P., 4th; Koche, R.; Saborowski, M.; Wilkinson, J.E.; Lowe, S.W. Arid1a Restrains Kras-dependent Changes in Acinar Cell Identity. *Elife* **2018**, *7*, e35216. [[CrossRef](#)]
61. Tentler, J.J.; Tan, A.C.; Weekes, C.D.; Jimeno, A.; Leong, S.; Pitts, T.M.; Arcaroli, J.J.; Messersmith, W.A.; Eckhardt, S.G. Patient-derived tumour xenografts as models for oncology drug development. *Nat. Rev. Clin. Oncol.* **2012**, *9*, 338–350. [[CrossRef](#)]

Disclaimer/Publisher’s Note: The statements, opinions and data contained in all publications are solely those of the individual author(s) and contributor(s) and not of MDPI and/or the editor(s). MDPI and/or the editor(s) disclaim responsibility for any injury to people or property resulting from any ideas, methods, instructions or products referred to in the content.